Multicarrier systems: a comparison between Filter Bank based and Cyclic Prefix based OFDM

Leonardo G. Baltar and Josef A. Nossek

Institute for Circuit Theory and Signal Processing
Technische Universität München, Germany
{leo.baltar,josef.a.nossek}tum.de

***Abstract*— In this contribution we perform a review of some recent developments and important results on Filter Bank based Multicarrier (FBMC) systems and make a comparison with Cyclic Prefix (CP) based OFDM. We first give an overview of the system structure and show how the subcarriers are generated. Then the spectral and peak-to-average power ratio (PAPR) behaviors are summarized. We review the subcarrier model used in the derivation of the per-subcarrier channel equalizers encountered in the recent literature and present a novel method of per-subcarrier channel estimation based on this same model. We finally compare the performance of both FBMC and CP-OFDM by showing some BER simulation results, where both systems occupy the same bandwidth and provide the same throughput. Even with channel estimation we can see that FBMC still achieves more than 1 dB of advantage in E_b/N_0 compared to CP-OFDM with a reasonable training sequence length.**

***Index Terms*— Multicarrier Systems, Filter Banks, OFDM, Filter Bank based Multicarrier.**

I. Introduction

OFDM is the most known multicarrier scheme to date and also the most employed in current standards for wireless communications [1]. But the multicarrier modulation concept of OFDM can be extended to the so-called Filter Bank based Multicarrier (FBMC) systems [2], [3]. OFDM is basically a particular implementation of a filter bank multicarrier system, where a trivial subcarrier filter with a rectangular impulse response is utilized transforming the filter bank into block-wise processing. These trivial subcarrier filter leads to out-of-band emissions, which decay very slowly due to the sinc-shaped spectra of the subcarriers. Since the propagation channel is usually frequency selective it inserts inter-symbol interference and the blocks of the OFDM system will overlap. To remove the block overlapping at the receiver, the OFDM data blocks will usually be preceded by a guard interval, the so-called Cyclic Prefix (CP). Some other guard intervals have been proposed in the literature without much success [4]. The CP has the advantage that the equalizers on a subcarrier level turn out to be very simple.

The minimum CP-length is determined by the length of the equivalent discrete-time channel impulse response. On the other hand CP-redundancy reduces both spectral efficiency and power efficiency. Therefore, the number of subcarriers (OFDM block length), which is associated with the duration of the OFDM-symbol should be as high as possible to limit the loss in efficiency. But this is in turn limited by the time-variance of the channel due to user mobility.

# Subcarriers	$\mathcal{C}_{\text{OFDM}}$	$\mathcal{C}_{\text{FB}}$	$\mathcal{A}_{\text{OFDM}}$	$\mathcal{A}_{\text{FB}}$
$M_{\text{FB}} = 1024$ $M_{\text{OFDM}} = 1024$	15	60	50	110
$M_{\text{FB}} = 256$ $M_{\text{OFDM}} = 1024$	15	98	50	138

TABLE I
NUMBER OF MULTIPLICATIONS AND ADDITIONS PER RECEIVED SYMBOL FOR FB MULTICARRIER AND CP-OFDM

With non-trivial subcarrier filters (e.g. root raised cosine filters in both synthesis and analysis filter banks) without any CP we increase spectral efficiency and reduce out-of-band emissions [5] at the cost of increased computational complexity.

The number of subcarriers in FBMC is mainly lower limited by the granularity needed for multi-user access and not because of spectral efficiency. With a lower number of subcarriers we achieve a lower peak-to-average power ratio (PAPR) at the transmitter output, which is essential for linear power amplifiers.

The complexity in number of real valued additions and multiplications per-multicarrier symbol is increased by the CP-less filter bank approach [6], see Table I. But this seems to be a good investment, where the return is reduced linearity required for the high power transmit amplifier and better usage of the scarce frequency resources.

This contribution is organized in the following structure: In Section II the basics of the FBMC are presented and the exponential modulation as well as the OQAM staggering are introduced. We shortly review the spectral and PAPR behavior of the FBMC system and compare to CP-OFDM in Section III. We present in Section IV the subcarrier model and review some important results

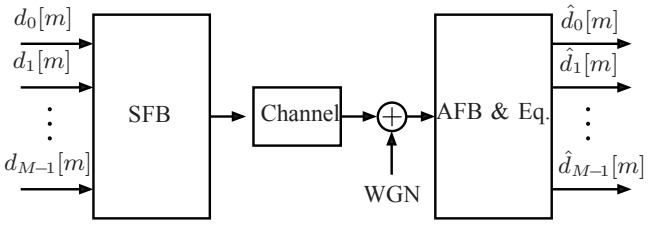

Fig. 1. FBMC System Overview.

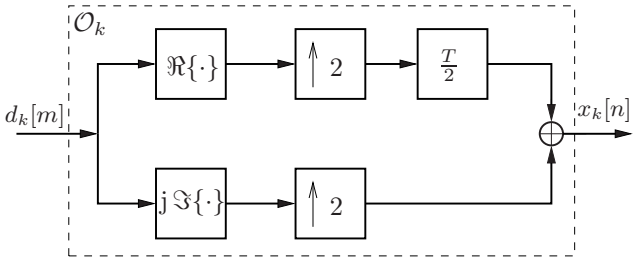

Fig. 2. O-QAM staggering for an even indexed subcarrier.

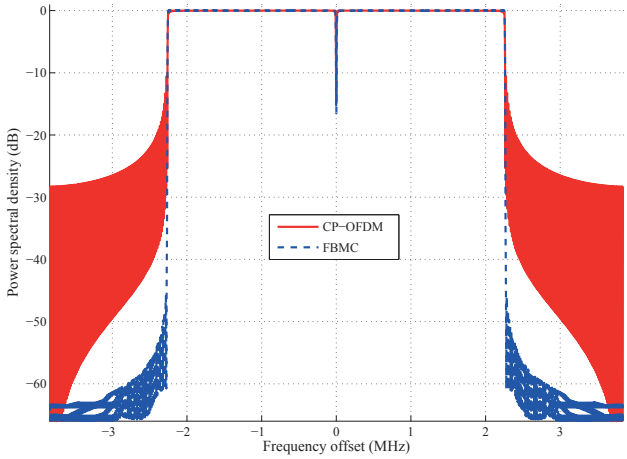

Fig. 3. Power Spectral density of FBMC and CP-OFDM.

on channel equalization. A novel per-subcarrier channel estimation method is introduced in Section V and simulation results comparing the performance of FBMC with CP-OFDM are presented in Section VI. In Section VII some conclusions are drawn.

II. FBMC System

A general overview of the FBMC system model is illustrated in Fig. 1. Here the filter banks are employed in a transmultiplex configuration [7]. At the transmitter a synthesis filter bank (SFB) performs a frequency division multiplexing (FDM) of the complex data symbols $d_k[m]$ into parallel subcarriers of rate $1/T$. At the receiver, an analysis filter bank (AFB) separates the data from the single subcarriers. In our model we include a frequency selective channel and an AWGN source between the SFB and the AFB. To really generate a band-limited broadband signal, only M_{u} out of the M subcarriers are filled with input signals, the rest remaining empty.

We consider here an exponentially modulated filter bank in both SFB and AFB. This means that only one prototype low-pass filter has to be designed and the other sub-filters are obtained by modulating it as follows

$$h_k[l] = h_0[l] \exp\left(\mathrm{j}\, 2\pi k l/M\right), \quad l = 0, \ldots, P-1, \quad (1)$$

where $h_0[l]$ is the impulse response of the prototype filter with length P and M is the total number of subcarriers. The prototype is a Nyquist-like filter usually with a roll-off factor $\rho = 1$ and as a consequence only contiguous subcarriers overlap in the frequency domain and non-contiguous subcarriers are separated by the good stop-band behavior. For example, a Root Raised Cosine filter (RRC) with length $P = KM + 1$ can be used, where K is the time overlapping factor that determines how many blocks of symbols superpose each other. K should be kept as small as possible in the first place to allow a low complexity and in the second place to reduce the spreading of the symbols in the time domain, specially in mobile environments.

Since the prototype filter is longer then the number of subcarriers M, and in order to maintain the orthogonality between all of them and for all time instants, the complex input symbols $d_k[m]$ need to have its real and complex parts staggered by $T/2$ resulting in an OQAM modulation scheme [8], [9], [2]. The OQAM staggering for even indexed subcarriers is depicted in Fig. 2. In odd indexed subcarriers the delay of $T/2$ is located at the lower branch with purely imaginary symbols. At the receiver the OQAM demodulation or de-staggering is performed by applying a flow-graph reversal [10] in Fig. 2, substituting the up-samplers by down-samplers and exchanging the blocks $\Re\{\cdot\}$ and $j\Im\{\cdot\}$.

After the OQAM staggering the signals of the different subcarriers are up-sampled by $M/2$, filtered and added. A broadband signal is then generated and after some eventual further digital processing, it is digital-to-analog (DA) converted to a baseband signal that will be then up-converted to RF and transmitted. At the receiver side the RF signal is brought to baseband, filtered and then analog-to-digital (AD) converted. The digital received signal is then filtered by the different analysis filters to generate the subcarrier signals.

III. Spectral and PAPR behavior

In Fig. 3 the power spectral density of both FBMC and CP-OFDM are depicted for a system with 5 MHz of bandwidth. Both systems have $M = 512$ subcarriers and the prototype filter is an RRC filter with length $P = KM+1$, where $K=4$. We can see that the out-of-band emissions of the FBMC system are much lower than the CP-OFDM. This enable the transmitter to fill more subcarriers with data, increasing the spectral efficiency and still fit a given spectral mask. It is also worth noting that any filter (digital or analog) that is to be applied after the MC modulation will have its requirements relaxed.

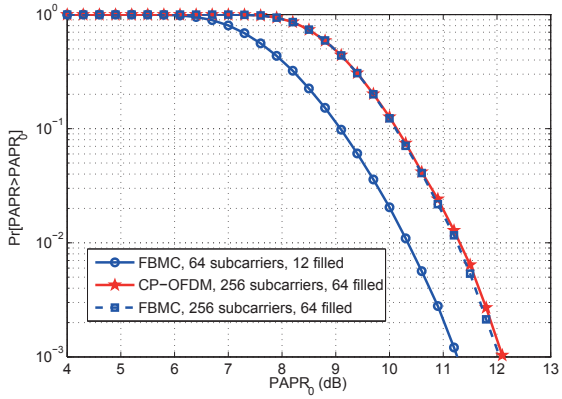

Fig. 4. Complementary Cumulative Distribution Function (CCDF) of the PAPR.

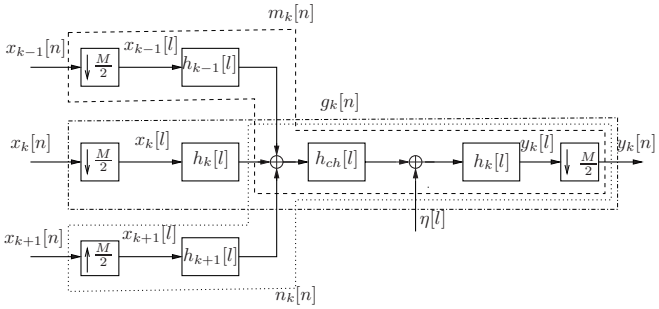

Fig. 5. Subchannel model.

One of the main drawbacks of CP-OFDM is the high PAPR behavior. This can also be observed in FBMC systems if we consider the complementary cumulative distribution function (CCDF) of the PAPR in Fig. 4. The curves represent the PAPR behavior for the multicarrier signals up-sampled by a factor of 4. As already mentioned, in FBMC, since the number of subcarriers is not constrained on the length of the channel impulse response, a reduction in the PAPR can be obtained if a lower number of subcarrier is employed in the same bandwidth. We can also see the CCDF of the PAPR in this case. Of course that an increased complexity of the channel estimation and equalization is expected in this case.

IV. Subcarrier model and Multi-tap Equalizer

Since we assume that only contiguous subcarriers overlap in the frequency domain, we can build the discrete-time subcarrier model shown in Fig. 5. The inputs $x_k[n]$ are the OQAM staggered symbols and the outputs are the received subcarrier signals $y_k[n]$ that still have to be equalized, since a frequency selective channel is assumed, and OQAM de-staggered before the QAM symbols are demodulated. As a consequence, in the subcarrier model the input and output sampling rate is $2/T$. We have assumed here perfect time and frequency synchronization. In other words, no time or frequency shifts (Carrier Frequency Offset or Doppler shift/spread) are present. A more realistic model would involve this and some other issues that are out of the scope of this contribution.

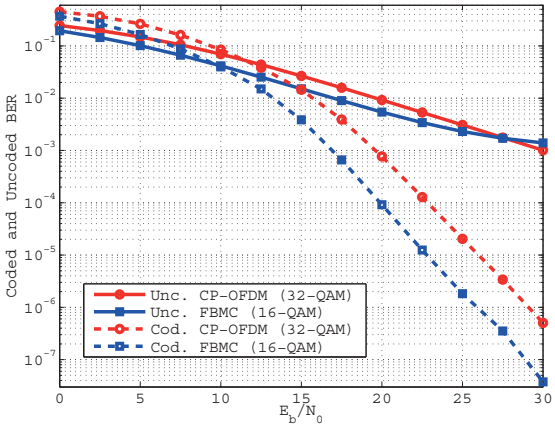

Fig. 6. Bit error rate for FBMC and CP-OFDM.

We collect N_o output symbols of the k-th subcarrier in an observation vector $\mathbf{y}_k[n] \in \mathbb{C}^{N_o}$. Then we express it as a function of the three input signals in subcarriers $(k–1)$, k and $(k+1)$ convolved with the impulse responses resulted from the down-sampling by $M/2$ of the convolution of transmit, receive filters and propagation channel, plus a thermal noise term. This leads us to the definition

$$\mathbf{y}_k[n] = \mathbf{G}_k\mathbf{x}_k[n] + \mathbf{M}_k\mathbf{x}_{k-1}[n] + \mathbf{N}_k\mathbf{x}_{k+1}[n] + \mathbf{\Gamma}_k\boldsymbol{\eta}[l], \quad (2)$$

where we have employed the convolution matrices $\mathbf{G}_k$, $\mathbf{M}_k$, $\mathbf{N}_k \in \mathbb{C}^{N_o\times(N_o+Q-1)}$, with $Q = \lceil\frac{2(P-1)+L_{ch}}{M/2}\rceil$, composed by the Q long impulse responses $g_k[n]$, $m_k[n]$ and $n_k[n]$. $\mathbf{\Gamma}_k \in \mathbb{C}^{N_o\times(P+\frac{M}{2}N_o)}$ is obtained by taking each $\frac{M}{2}$-th row of the convolution matrix composed by the analysis filter impulse response $h_k[l]$.

The frequency selective propagation channel will introduce temporal ISI and inter-carrier interference (ICI) in the received symbols, turning equalization into a more sophisticated issue as compared to CP-OFDM. To reduce the bit-error-ratio after the demodulation of the received symbols the equalizer has to be introduced before the OQAM de-staggering. A per-subcarrier fractionally spaced linear MMSE or DFE MMSE equalizer can be employed for this matter as it can be found in [11], [12], where the same subcarrier model as presented here was used. But before the equalizers can be designed a channel estimation in a per-subcarrier basis has to be performed and this topic will be covered in the next section. An example of the per-subcarrier equalizer performance when perfect channel knowledge at the receiver side was assumed is shown in Fig. 6. A comparison of the uncoded and coded BER for FBMC and CP-OFDM is shown for the case where both systems have the same throughput. This example was taken from [13]. It can be observed the advantage of FBMC of 2.5 dB in E_b/N_0 in the coded case.

We should mention here that there are efficient realizations for the subcarrier filtering operation. In this case, the

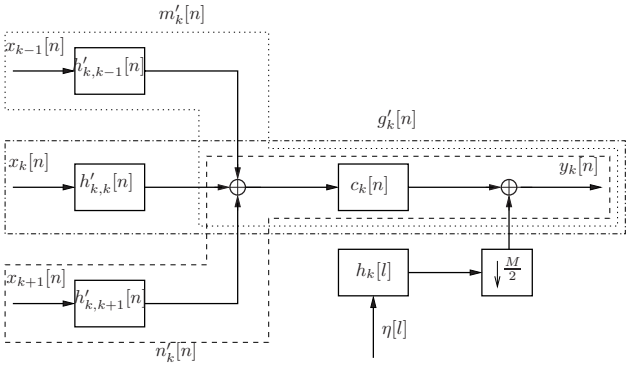

Fig. 7. Modified subcarrier model for structured approach.

modulation of the prototype filter to generate each subfilter is performed with the help of the Fast Fourier Transform. In order to perform the filtering in a lower sampling rate, the polyphase decomposition [7] of the prototype filter is also employed. Those efficient realizations can be found, for example, in [9].

V. Structured Subcarrier Channel Estimation

To perform the structured subcarrier impulse response estimation we have first to modify the subcarrier model. The idea is to model the propagation channel viewed from the receiver side at each subcarrier as a narrow-band FIR filter with a short impulse response and represent it in a lower sampling rate, namely the double of the symbol rate or $2/T$. For this we first convolve the transmit filters $h_{k-1}[l]$, $h_k[l]$ and $h_{k+1}[l]$ with the receive filter $h_k[l]$ and down-sample by $M/2$. The resulting impulses $h'_{k-1}[n]$, $h'_k[n]$ and $h'_{k+1}[n]$ have length $Q_\mathrm{f} = \lceil \frac{2P-1}{M/2} \rceil$. As a consequence the narrow-band propagation channel experienced by subcarrier k has the impulse response $c_k[n]$. The three new overall impulse responses for the contiguous subcarriers are $g'_k[n] = h'_k[n] * c_k[n]$, $m'_k[n] = h'_{k-1}[n] * c_k[n]$, $n'_k[n] = h'_{k-1}[n] * c_k[n]$ and have length $Q_\mathrm{f}+L_\mathrm{c}-1$, where L_c is the length of the impulse response $c_k[n]$. This new subcarrier model is illustrated in Fig. 7.

We can now express the output of one subcarrier as

$$\mathbf{y}_k[n] = \mathbf{G}'_k\mathbf{x}_k[n] + \mathbf{M}'_k\mathbf{x}_{k-1}[n] + \mathbf{N}'_k\mathbf{x}_{k+1}[n] + \mathbf{\Gamma}_k\boldsymbol{\eta}[l], \tag{3}$$

with convolution matrices $\mathbf{G}'_k$, $\mathbf{M}'_k$, $\mathbf{N}'_k \in \mathbb{C}^{N_\mathrm{o}\times(N_\mathrm{o}+Q_\mathrm{f}+L_\mathrm{c}-1)}$.

Now we rewrite (3) by stacking the impulse responses in vectors and arranging the input training sequences in matrices. The observation vector can be expressed as

$$\mathbf{y}_k[n] = \mathbf{X}_k[n]\mathbf{g}'_k + \mathbf{X}_{k-1}[n]\mathbf{m}'_k + \mathbf{X}_{k+1}[n]\mathbf{n}'_k + \mathbf{\Gamma}_k\boldsymbol{\eta}[l], \tag{4}$$

where $\mathbf{g}'_k$, $\mathbf{m}'_k$ and $\mathbf{n}'_k \in \mathbb{C}^{Q_\mathrm{f}+L_\mathrm{c}-1}$ contain the impulse reponses $g'_k[n]$, $m'_k[n]$ and $n'_k[n]$ that result from the convolution of the down-sampled sub-filters and the narrowband propagation channel. $\mathbf{X}_k[n], \mathbf{X}_{k-1}[n], \mathbf{X}_{k+1} \in \mathbb{C}^{N_\mathrm{o}\times(Q_\mathrm{f}+L_\mathrm{c}-1)}$ are Hankel matrices containing the OQAM-staggered input training sequences that have length $N_\mathrm{t} = \lceil \frac{N_\mathrm{o}+Q_\mathrm{f}+L_\mathrm{c}-1}{2} \rceil$. It is important to note here the difference to Equation (2). In that model the impulse responses $g_k[n]$, $m_k[n]$ and $n_k[n]$ were obtained after the convolution between transmit sub-filters, broadband propagation channel and receive sub-filter, and then down-sampling the resulting impulse responses by $M/2$. Moreover, by assuming a training sequence with length N_t as defined before, the observations contained in $\mathbf{y}_k[n]$ are completely independent of the data symbols following the training sequences. This requisite could be relaxed but some loss in performance would be expected.

It is clear that the components of vectors $\mathbf{g}'_k$, $\mathbf{m}'_k$ and $\mathbf{n}'_k$ depend on the narrowband propagation channel model, but also on the known transmit and receive filters. If we separate both impulse responses we can write $\mathbf{g}'_k = \mathbf{H}_{k,k}\mathbf{c}_k$, $\mathbf{m}'_k = \mathbf{H}_{k,k-1}\mathbf{c}_k$ and $\mathbf{n}'_k = \mathbf{H}_{k,k+1}\mathbf{c}_k$, where $\mathbf{H}_{k,k}, \mathbf{H}_{k,k-1}, \mathbf{H}_{k,k+1} \in \mathbb{C}^{(Q_\mathrm{f}+L_\mathrm{c}-1)\times L_\mathrm{c}}$ and $\mathbf{c}_k \in \mathbb{C}^{L_\mathrm{c}}$ is a vector containing the impulse response $c_k[n]$. As a consequence, the received signal is now given by

$$\begin{aligned}\mathbf{y}_k[n] &= (\mathbf{X}_k[n]\mathbf{H}_{k,k} + \mathbf{X}_{k-1}[n]\mathbf{H}_{k,k-1} \\ &\quad + \mathbf{X}_{k+1}[n]\mathbf{H}'_{k,k+1})\mathbf{c}_k + \mathbf{\Gamma}_k\boldsymbol{\eta}[l] \\ &= \mathbf{S}_k\mathbf{c}_k + \mathbf{\Gamma}_k\boldsymbol{\eta}[l].\end{aligned} \tag{5}$$

We can note that the length L_c of $\mathbf{c}_k$ is a design parameter of the channel estimator. L_c can be different for different subcarriers depending on how frequency selective the propagation channel is for a certain frequency region. The estimation of $\mathbf{c}_k$ is called in the literature structured channel estimation [14], because $\mathbf{S}'_k$ depends on the training sequences and on the filters at transmitter and receiver side. We can see that in the linear model of (5) the noise is zero mean Gaussian distributed with autocorrelation matrix $\mathbf{R}_{\eta,k} = \sigma_\eta^2\mathbf{\Gamma}_k\mathbf{\Gamma}_k^\mathrm{H}$ and the observation $\mathbf{y}_k[n]$ given $\mathbf{c}_k$ is Gaussian distributed. The maximum likelihood (ML) estimate of $\mathbf{c}_k$ in this case is given by

$$\hat{\mathbf{c}}_{k,\mathrm{ML}} = \arg\max_{\mathbf{c}_k} p(\mathbf{y}_k[n]|\mathbf{c}_k). \tag{6}$$

Since $\mathbf{R}_{\eta,k}$ is independent of $\mathbf{c}_k$ and $(\mathbf{S}_k^\mathrm{H}\mathbf{R}_{\eta,k}^{-1}\mathbf{S}_k)$ is invertible, the ML estimate of the subcarrier impulse response is given by

$$\begin{aligned}\hat{\mathbf{c}}_k &= (\mathbf{S}_k^\mathrm{H}\mathbf{R}_{\eta,k}^{-1}\mathbf{S}_k)^{-1}\mathbf{S}_k^\mathrm{H}\mathbf{R}_{\eta,k}^{-1}\mathbf{y}_k[n] \\ &= (\mathbf{S}_k^\mathrm{H}(\mathbf{\Gamma}_k\mathbf{\Gamma}_k^\mathrm{H})^{-1}\mathbf{S}_k)^{-1}\mathbf{S}_k^\mathrm{H}(\mathbf{\Gamma}_k\mathbf{\Gamma}_k^\mathrm{H})^{-1}\mathbf{y}_k[n] \\ &= \mathbf{W}_k\mathbf{y}_k[n].\end{aligned} \tag{7}$$

It is worth to mention that the matrices $\mathbf{W}_k$ are computed off-line given a prototype filter and the training sequences in the three contiguous subcarriers. This means that the complexity of the channel estimation during the demodulation process is given by the product $\mathbf{W}_k\mathbf{y}_k[n]$, resulting in $L_\mathrm{c} \times N_\mathrm{o}$ multiplications and $L_\mathrm{c} \times (N_\mathrm{o}-1)$ additions per subcarrier.

VI. Channel Estimation Performance Comparison

To compare the performance of FBMC with CP-OFDM in a multi-path propagation environment we have done Monte-Carlo simulations in MATLAB. We have assumed

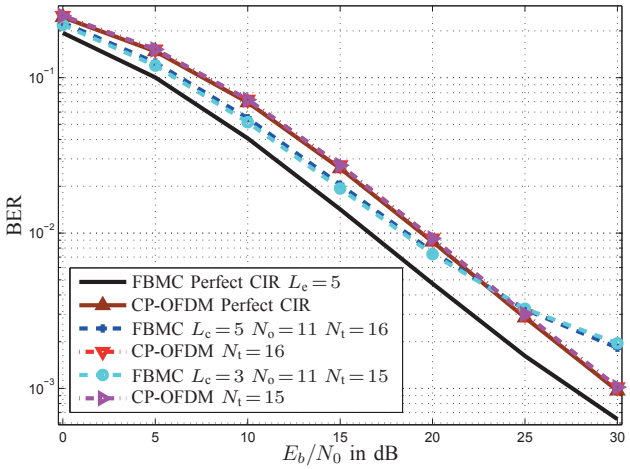

Fig. 8. BER comparison, $M = 256$ subcarriers, $M_u = 210$, 10 MHz, ITU Veh. A.

a bandwidth of 10 MHz and a sampling rate of 11.2 MHz, both systems have a total of $M = 256$ subcarriers available but only $M_u = 210$ are filled and we considered a static channel with the power delay profile of the ITU Veh. A. The resulting subcarrier distance is 43.75 kHz. The prototype filter is a RRC with length $P = KM + 1$, where $K = 4$.

We have employed the per-subcarrier unbiased MMSE equalizer with length L_e for FBMC and the zero forcing equalizer for CP-OFDM. In the latter system the length of the CP was $L_{CP} = 64$ and that is $1/4$ of the OFDM symbol length. Again to maintain the same throughput we have used a 16-QAM alphabet for FBMC and 32-QAM for CP-OFDM.

We also compare the quality of the channel estimation. For this we have used a randomly generated training sequence with symbols taken from a QPSK alphabet. We employed the same training sequence length for both systems, in the FBMC system the structured ML channel estimator presented in the previous section was used and in CP-OFDM a per-subcarrier LS channel estimator given by

$$c_k = \frac{\sum_i^{N_t} x_k[n-i]^* y_k[n-i]}{\sum_i^{N_t} x_k[n-i]^* x_k[n-i]} \tag{8}$$

was used.

In Fig. 8 the BER curves for both FBMC and CP-OFDM are presented for 200 channel realizations and $N_b = 1000$ symbols per-subcarrier for each channel realization. We can see the advantage of almost 3 dB less energy per bit necessary in the middle SNR regime for the same BER for FBMC compared to CP-OFDM when perfect channel knowledge is assumed at the receiver side. In the case of estimated channels with a still reasonable number of training symbols the gain achieved is more 1 dB in the middle SNR regime. It is worth mention that in this simulations the training symbols were not optimized for the systems under evalution. With optimal training sequences some gain in performance is expected for the same training length.

VII. Conclusions

We have presented a review of some important results and a comparison between FBMC and CP-OFDM system. We have also presented a novel scheme for the channel estimation of the subcarrier impulse response. From the simulation results we could see that the FBMC system still can achieve a gain of more than 1 dB in E_b/N_0 over CP-OFDM when the receiver has to estimate the subcarriers impulse response and a per-subcarrier MMSE equalizer is employed. It is worth mentioning that no optimal training sequence was used and the results could be even improved in that case.

References

[1] J. A. C. Bingham, "Multicarrier modulation for data transmission: an idea whose time has come," *IEEE Comm. Mag.*, vol. 28, no. 5, pp. 5–14, 1990.

[2] Pierre Siohan, Cyrille Siclet, and Nicolas Lacaille, "Analysis and design of OFDM/OQAM systems based on filterbank theory," *IEEE Trans. on Signal Processing*, vol. 50, no. 5, pp. 1170–1183, May 2002.

[3] B. Farhang-Boroujeny, "OFDM versus filter bank multicarrier," *IEEE Sig. Process. Mag.*, vol. 28, no. 3, pp. 92–112, 2011.

[4] Heidi Steendam and Marc Moeneclaey, "Different guard interval techniques for ofdm: Performance comparison," in *in Proc. of MC-SS 07*, 2007, pp. 7–9.

[5] L. G. Baltar, D.S. Waldhauser, and J.A. Nossek, "Out-of-band radiation in multicarrier systems: A comparison," in *Multi-Carrier Spread Spectrum 2007*, Simon Plass, Armin Dammann, Stefan Kaiser, and Khaled Fazel, Eds., vol. 1 of *Lecture Notes in Electrical Engineering*, pp. 107–116. Springer Netherlands, 2007.

[6] L. G. Baltar, F. Schaich, M. Renfors, and J. A. Nossek, "Computational complexity analysis of advanced physical layers based on multicarrier modulation," in *Proc. Future Network & Mobile Summit (FutureNetw)*, June 2011, pp. 1–8.

[7] P. P. Vaidyanathan, *Multirate Systems and Filter Banks*, Prentice-Hall, Englewood Cliffs, NJ, 1993.

[8] Burton R. Saltzberg, "Performance of an efficient parallel data transmission system," *IEEE Trans. Communication Technology*, vol. COM-15, no. 6, pp. 805–811, December 1967.

[9] T. Karp and N.J. Fliege, "Modified DFT filter banks with perfect reconstruction," *Circuits and Systems II: Analog and Digital Signal Processing, IEEE Transactions on*, vol. 46, no. 11, pp. 1404–1414, Nov. 1999.

[10] Schafer R.W. Buck J.R. Oppenheim, A.V., *Discrete-Time Signal Processing*, Prentice-Hall, Upper Saddle River, NJ, EUA, second edition, 1997.

[11] L. G. Baltar, D. S. Waldhauser, and J. A. Nossek, "MMSE subchannel decision feedback equalization for filter bank based multicarrier systems," in *Proc. IEEE Int. Symp. Circuits and Systems ISCAS 2009*, 2009, pp. 2802–2805.

[12] D. S. Waldhauser, L. G. Baltar, and J. A. Nossek, "Adaptive equalization for filter bank based multicarrier systems," in *Proc. IEEE Int. Symp. Circuits and Systems ISCAS 2008*, 2008, pp. 3098–3101.

[13] L. G. Baltar, A. Mezghani, and J. A. Nossek, "MLSE andMMSE subchannel equalization for filter bank based multicarrier systems: Coded and uncoded results," in *Proceedings of the 18th European Signal Processing Conference (EUSIPCO-2010)*, Aalborg, Denmark, August 2010, pp. 2186–2190.

[14] Boon Chong Ng, M. Cedervall, and A. Paulraj, "A structured channel estimator for maximum likelihood sequence detection in multipath fading channels," *Vehicular Technology, IEEE Transactions on*, vol. 48, no. 4, pp. 1216 –1228, jul 1999.